ELSEVIER

Journal of Power Sources 79 (1999) 1–8

JOURNAL OF POWER SOURCES

Electrochemical characteristics of binary silver alloys in alkaline solution

Tomislav D. Grozdić [a], Dragica Lj. Stojić [b,*]

[a] University of Belgrade, PO Box 550, 11 001 Belgrade, Yugoslavia
[b] The Institute of Nuclear Sciences Vinča, Department of Physical Chemistry, PO Box 522, 11 001 Belgrade, Yugoslavia

Received 4 July 1997; received in revised form 24 August 1998

Abstract

The electrochemical features, electrode capacity and corrosion stability, of silver alloys with Tl, Pb, P, Sb, Ge and In have been investigated. Compared to silver some silver alloys showed improved silver oxide formation and conductivity. The best effects, i.e., dramatic increases of 150% for formation of oxide, were obtained with small amounts of alloying component: 0.44% Tl or 0.44% Pb. Based on obtained results, those effects could be explained in terms of increase of real electrode surface as a consequence of ingredients oxidation, preceding the silver oxidation. © 1999 Elsevier Science S.A. All rights reserved.

Keywords: Silver alloys; Oxide formation; Charge capacity; Real surface; Corrosion stability

1. Introduction

In general, the application of Ag–Zn batteries requires the high rate capability and long discharge times. These features can be achieved when oxide formation, i.e., charge acceptance, and electric conductivity become improved, the electrode porosity increased, etc.

The semiconducting feature of Ag_2O layer upon a silver substrate itself suggests those small amounts of ingredients, incorporated as the alloying component, contribute to a dramatic increase of oxide formation [1] and probably to its conductivity.

The charge acceptance of Ag was increased up to 20% with addition of 1–1.5% Pd [2,3] and Au (up to 10%) [4,5], although Au, Sn and Pb (at 2% level) [5] accelerates the decomposition of AgO to Ag_2O [5]. No effects were noticed with addition of 2% Th, 1% In, As and Sn, and Se (trace concentration). For Ag alloys with Bi [5] no effects were observed with addition of 5% Pd and 10% Zn [6], although Zn tends to corrode the electrode surface and affects the oxide potential. The charge acceptance was lowered with addition of 20% Cd [6], 10% Pt and combined addition of Te and Sb (at 2% level) [5]. Increased charge acceptance could also be achieved by alloying silver with In, Tl, Pb, as it is shown in the Refs. [1,7,8].

The main leading idea of this work has been to increase the formation of silver oxide on a silver electrode. One approach was to make silver alloys with Tl, Pb, P, Sb, Ge and/or In. An attempt was also made to explain the noticed effects of improved charge acceptance.

2. Experimental

Electrochemical measurements of electrode charge and discharge processes were carried out in a classic electrochemical cell made of glass (300 cm^3) with nickel as the counter electrode and Hg/HgO as the reference electrode (+95 mV vs. NHE). Electrolyte was 1 mol dm^{-3} KOH. Working electrode, silver or silver alloys, was in contact with reference electrode over Luggin capillary. All experiments were made in nitrogen atmosphere, purified over copper turnings and molecular sieves, and bubbling through the solution preceding each experiment.

Silver and its alloys as working electrodes, were made of corresponding high purity metals. Silver purity was 99.9% and for all other components the purity was as follows: 99.99% In, 99.95% Tl, 99.99% Pb, 99.98% Sb and 99.4% P. Granulated silver ($r = 1.5$ mm) and the alloying component, cut into the particles with a maximum diameter of 0.5 mm, were mixed mechanically. Each mixture was placed into a quartz ampulla (diam. 18 mm) with charcoal on the top of the mixture and heated in acetylene flame up to its melting point. After 5 min of heating, ampulla was immediately dipped into the water.

* Corresponding author. Fax: +381-011-453-967; E-mail: estojicd@rt270.vin.bg.ac.yu

0378-7753/99/$ - see front matter © 1999 Elsevier Science S.A. All rights reserved.
PII: S0378-7753(98)00160-8

The shape of silver alloy, obtained in such a way, was cylindrical ($H = 40$ mm, $r = 18$ mm).

The silver plate (pure and/or alloyed electrodes) were masked with an acrylic resin to leave an exposed apparent area of 0.25 cm^2 and 0.1 cm^2, respectively. All electrodes, including pure silver, were mechanically polished by successively finer grade of emery papers and then by alumo-particles (alumina 1, 0.3 and 0.05 μm).

Before a metallographic characterization, the surface of every specimen was etched with cyanide or bichromate solution. Bichromate solution represents a very poor etching reagent for silver and silver alloys. The cyanide solution composition: 50 cm^3 5% KCN and 50 cm^3 5% ammonium–persulphate. The surface was etched for about 1–2 min. The bichromate solution content was the following: 100 cm^3 $K_2Cr_2O_7$, 2 cm^3 saturated solution of NaCl and 900 cm^3 distilled H_2O. The surface was also etched for about 1–2 min.

2.1. Physico-chemical measurements

Lead and thallium content in silver alloys and in the electrolyte was determined by emission spectroscopy using Quantoscan, ICP, 3500 ARL (Switzerland).

Metallographic photographs sample surface were obtained using Versamat metallograph, Union 6527, Buhler (USA).

Distribution of alloying components were detected by Electronic microscope AEI, microsond SEM-2 (G.B.).

A surface area of a plain electrode was determined by Hg-poremeter Carlo Erba M2000 (Italy).

2.2. Electrochemical measurements

2.2.1. The galvanostatic method

In the galvanostatic method, current of a test electrode was adjusted to a specific value that can be kept constant for a long time by galvanostat (PAR Galvanostat/Potentiostat Model 173). The potential was recorded on Y-t recorder (2000 Omnigrafic, Houston).

3. Results

In our experiments the following electrodes were tested: Ag-pure, Ag-0.044% Tl, Ag-0.44% Tl, Ag-0.044% Pb, Ag-0.44% Pb, Ag-0.26% In, Ag-1.10% In, Ag-0.28% Sb, Ag-0.03% Ge, and Ag-0.66% P.

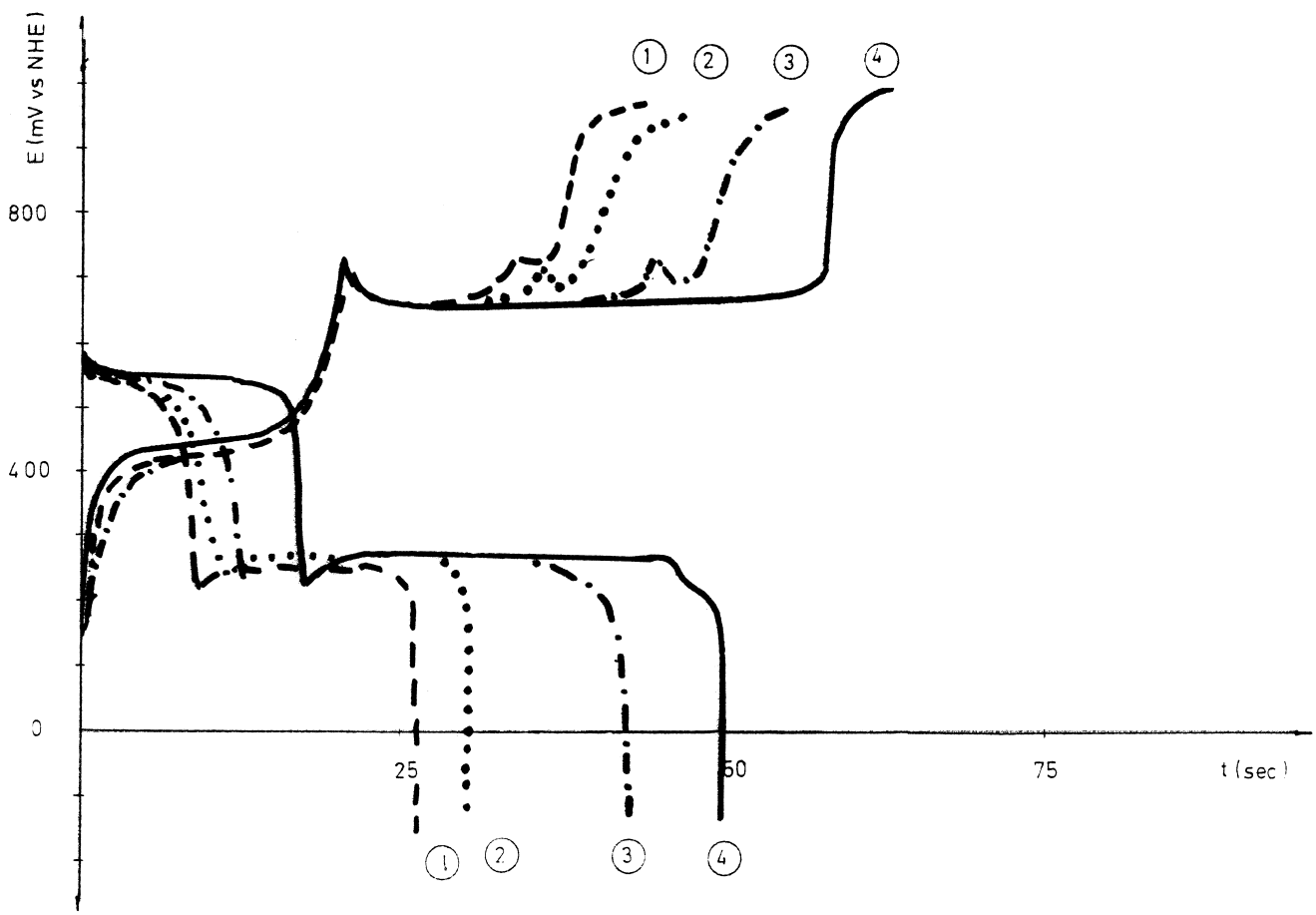

Fig. 1. Galvanostatic curve for charge and discharge of silver electrode, $i_{charge} = i_{discharge} = 5$ mA cm^{-2}.

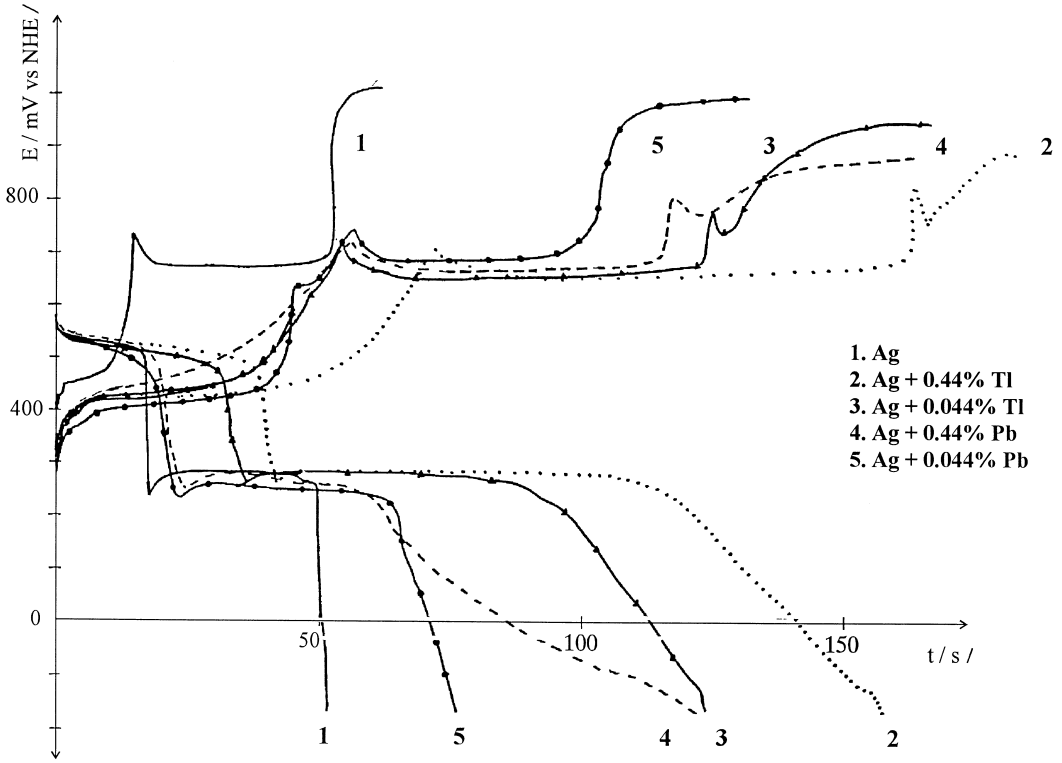

Fig. 2. Galvanostatic curve for charge and discharge of binary alloy silver electrodes when alloying components are Tl and Pb, $i_{charge} = i_{discharge} = 5$ mA cm^{-2}.

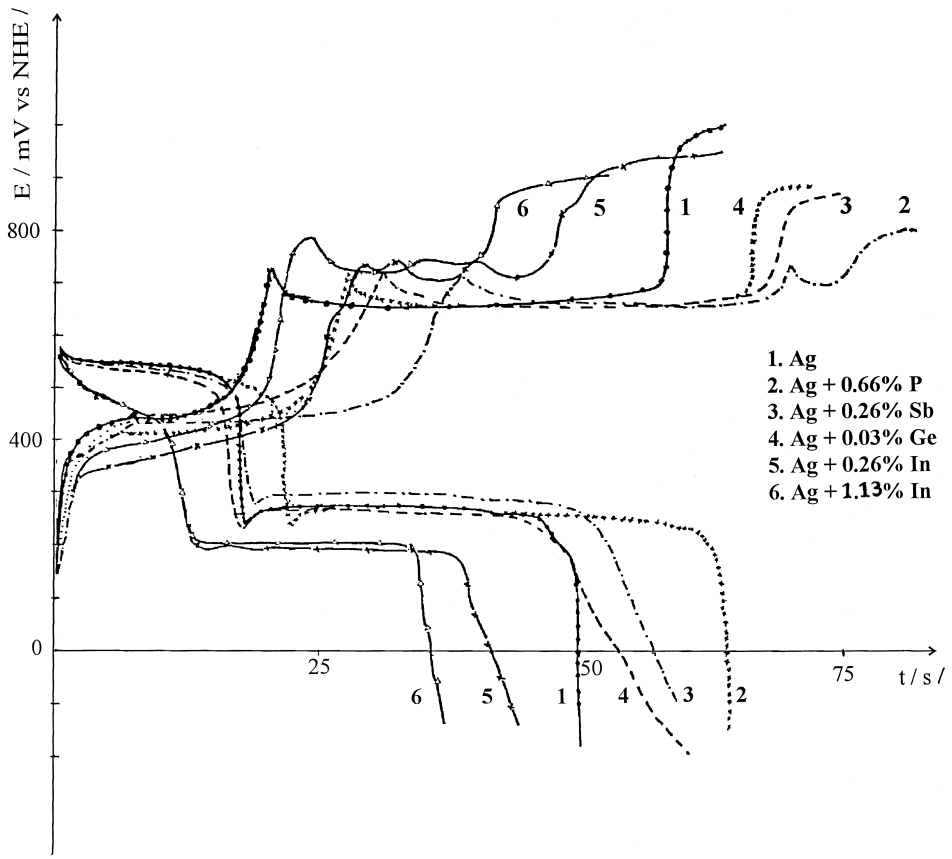

Fig. 3. Galvanostatic curve for charge and discharge of binary alloy silver electrode when alloying component are P, Sb, Ge, In, $i_{charge} = i_{discharge} = 5$ mA cm^{-2}.

All contents are in weight percent.

For electrodes that gave the best results, Ag-0.44% Tl and Ag-0.44% Pb, the content of alloying component was determined by emission spectroscopy. The contents obtained were as follows: Ag-0.71% Tl and Ag-0.26% Pb.

All electrodes were charged and discharged galvanostatically with constant current density, $i = 5$ mA cm^{-2}. The discharging curves were satisfactory reproductive after 6–7 cycles. First charging and discharging curves have the same shape as the second and following curves and only capacity appears changed, i.e., increased (see Fig. 1). This is the reason that first cycles are not shown for all other electrodes. The results obtained after 6–7 charging and discharging cycles are shown in Figs. 2 and 3. The charging curve for a pure silver electrode has two plateaus. It is generally agreed that the first plateau is associated with the formation of Ag_2O and arises short because a layer of Ag_2O, only about three molecules thick, is formed before the potential rise to the second plateau [2]. The new electrode process represents the formation of AgO taking place at the potential of the second plateau. Second plateau is preceded by potential peak (the potential peak usually precedes to the plateau). Finally, at the end of the second plateau, the potential rises to a steady value of O_2 evolution.

The shape of charging curves for each alloy electrode is very similar to the shape for pure silver (see Figs. 2 and 3). The peaks arising at the beginning of oxygen evolution, existing on some charging curves for each alloy electrode, are also noticed for the pure silver itself [2]. After the silver electrode had been anodized to the point of O_2 evolution, the current was reversed and the constant current discharging curve is also shown in Figs. 2 and 3. As soon as the current is applied, the potential falls to a short plateau at the Ag_2O/AgO potential. The length of this Ag_2O/AgO plateau becomes shorter as the current density increases. With time elapsing, the potential falls to Ag/Ag_2O potential, where it remains until the whole oxide becomes reduced. After that, at very negative potential values, the system shifts quickly to the evolution of H_2. Silver–thallium alloys have a rather high capacity. With the large content of thallium 0.44%, the influence on its capacity is higher and this alloy has the highest discharge capacity, see curve 3 (Fig. 2). Lead contents of 0.44% and 0.044% also has a positive effect (see curves 4 and 5, Fig. 2). Other alloys with P, Sb and Ge also have a positive effect (see Fig. 3) but not so pronounced as alloys with thallium (Fig. 3, curves 2 and 3). The capacity of indium alloys is lower then for pure silver (see curves 5 and 6, Fig. 3) that means that indium as an alloying

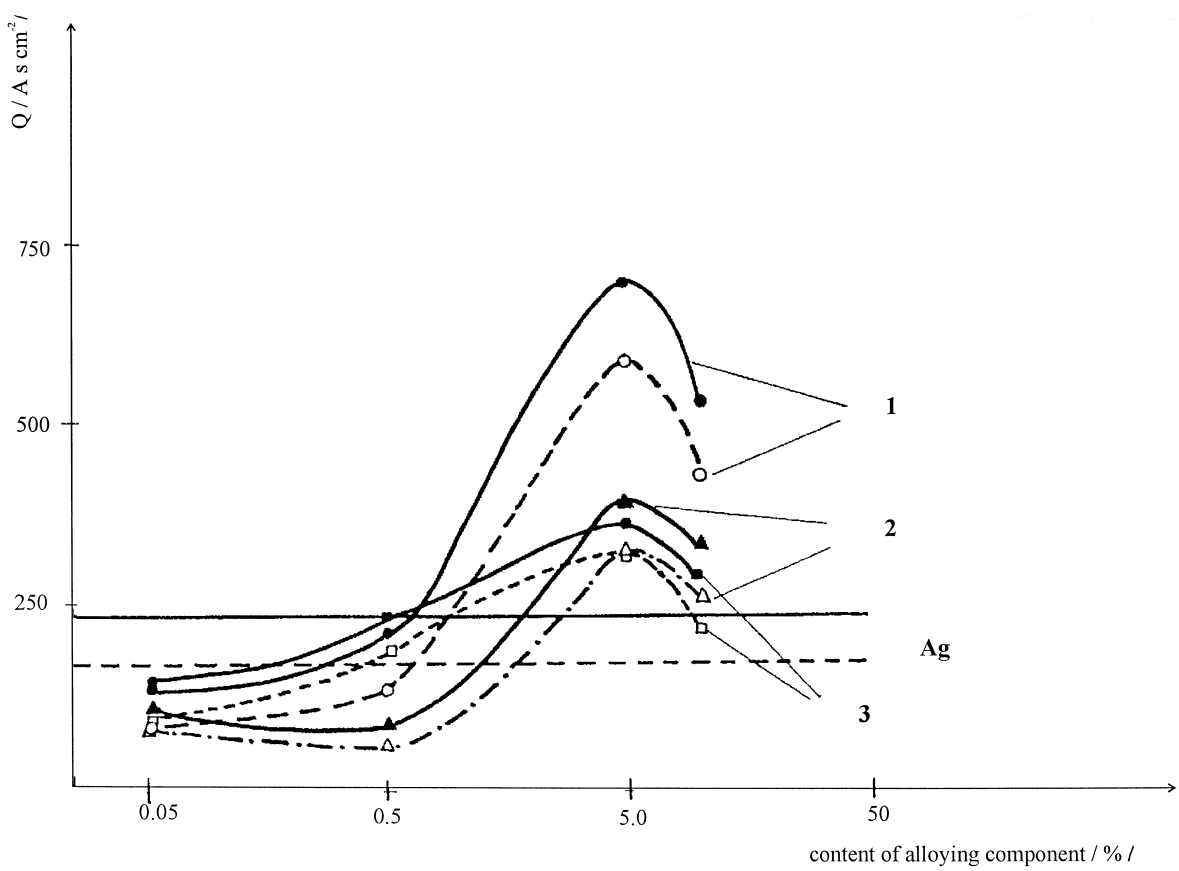

Fig. 4. Capacity of charge (————) and discharge (- - -) of alloyed silver electrodes vs. content of alloying component, $i_{charge} = i_{discharge} = 5$ mA cm^{-2}. Ag–Pb (curve 1), Ag–In (curve 2), Ag–Tl (curve 3) and pure silver (parallel to X-axis).

component exhibits a negative influence. Finally, the electrodes can be ordered in decreasing capacity order in the following way: Ag-0.44% Tl > Ag-0.044% Tl > Ag-0.44% Pb > Ag-0.044% Pb > Ag-0.66% P > Ag-0.26% Sb > Ag-0.03% Ge > Ag > Ag-0.26% In > Ag-1.10% In.

The current density was calculated according to the geometrical surface of an electrode. However, the real surface of an electrode arises increasing after several charge–discharge cycles. A real surface of an electrode after seven cycles was measured and found increased for three times. Further cycling has no influence to the electrode surface.

The electrode capacity values for electrode charging and discharging processes vs. content of alloying components is shown on the diagram (see Fig. 4). Horizontal and dashed lines on that diagram show the capacity of pure silver. Electrode capacity of alloys Ag–Tl and Ag–Pb, with alloying components in contents less than 0.5%, decreases in comparison to the capacity of pure silver electrode and Ag–In alloy. However, higher contents of those ingredients produce the remarkable increase in the electrode capacity. The highest capacity of an electrode has been reached with addition of 1–5% Pb. Further increases in Tl and Pb content affect the electrode capacity to decrease. Ag–In alloys show highest increase of the capacity in a range of 2–5%, and after that the electrode capacity decreases.

The good corrosion stability of an oxide electrode is of a substantive interest. Only a stable enough oxide electrode can be applied in a battery cell. A test of oxide stability in the present electrolyte is carried out with the electrode charged at constant current density of 5 mA cm^{-2}. The stationary potential is measured as a function of time (current $I = 0$). The stationary potential for Ag–Tl alloys and pure silver vs. time is shown in Fig. 5. Obviously, the shape of curve is almost the same as the discharging curve for pure silver. Alloys Ag-10% Tl and Ag-5% Tl appear self-discharged before an electrode of pure silver. Alloy Ag-0.05% Tl behaves self-discharging at the same time as electrode of pure silver. Ag-0.5% Tl electrode is discharged more slow than all other electrodes.

Generally, during the self-discharging process, chemical decomposition of silver(II)oxide and than the formation of silver(I)oxide mainly occurs. Time for self-discharge of Ag–In and Ag–Pb electrode vs. content of alloying component is shown in Fig. 6. The stationary potential is measured as a function of time (current $I = 0$). Ag–In with content 0.1–4.5% have higher self-discharging rate than pure silver. The Ag–Pb alloy, only with content 0.5-1% Pb, behaves similar self-discharge as pure silver.

The effect of increased capacity by alloying silver with Tl, In or Pb is attempted to explain. For the sake of explanation of the phenomenology of alloying effect, is interesting to compare voltammograms for pure polycrystalline silver with Ag-0.44% Tl and pure thallium (see Fig. 7). The potential scan range and sweep rate were from −1100 to +920 mV NHE and 2 mV s^{-1}, respectively. Voltammogram for pure silver generally shows five peaks

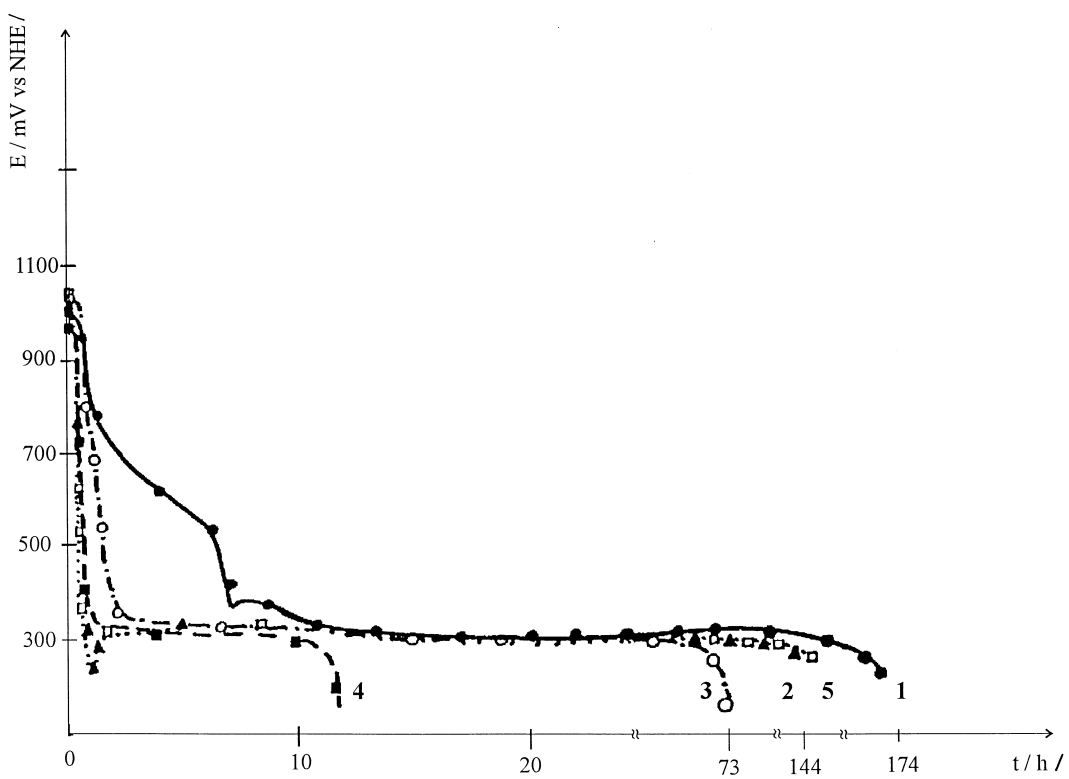

Fig. 5. Stationary potential of alloyed silver electrodes vs. decay time ($I = 0$). Ag-0.5% Tl (curve 1), Ag-0.05% Tl (curve 2), Ag-5% Tl (curve 3), Ag-10% Tl (curve 4) and pure silver (curve 5).

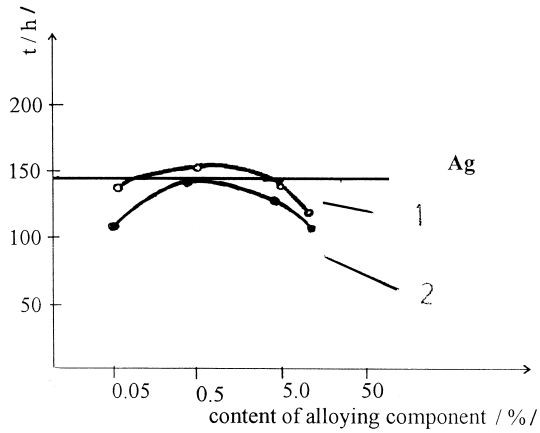

Fig. 6. Time for self-discharge of Ag–In (curve 1) and Ag–Pb (curve 2) electrode vs. content of alloying component ($I = 0$). Self-discharge of a pure silver electrode is shown with parallel line to X-axis.

in the anodic and five reduction peaks in the cathodic sweep. There is general agreement in the literature [2,3] that two major anodic and cathodic peaks are related to the formation of Ag_2O and AgO, and to the reduction of AgO and Ag_2O [2]. The peak before the main Ag_2O formation has usually been attributed by many authors to the formation of Ag(OH) [2].

During a complete cycle, the total oxidation and reduction charges were identical, demonstrating that practically all oxidation products remain on the electrode.

Voltammogram for pure thallium has peaks only in the negative potential range. One peak at −580 mV NHE is formed during the anodic sweep scan and, at the positive potential region, the current density is almost (equal to) zero. During the cathodic sweep, there appears the reduction peak for a thallium ion. Obviously, drastic dissolution and corrosion of thallium occurs during the anodic sweep. That could be proved by the visual observation of the surface of a plain electrode. The surface arises completely ruined and has many deep holes.

The shape of the curve for Ag-0.44% Tl electrode is very similar to the one for pure silver in a positive potential range. However, the curve for the alloyed electrodes in a negative potential range from −400 to −1000 mV NHE has two peaks more during the anodic and cathodic sweeps than curve for pure silver. The shapes of the curves for alloy and pure silver are similar. Silver oxide formation in Ag–0.44% Tl occurs prior to the same for a pure silver electrode, i.e., the oxidation peak is being shifted for 10–20 mV to more negative potentials. The reduction of silver oxide is shifted for 10–20 mV to the negative potential also. Oxygen evolution is also increased on Ag-0.44% Tl electrode in comparison to the pure silver electrode. It is obvious from the first glance of voltammogram that area under oxygen evolution peak for the silver alloys is larger than area for pure silver.

In the case of Ag-0.26% In alloy the oxidation peak for Ag_2O is shifted for 40 mV to the negative potential

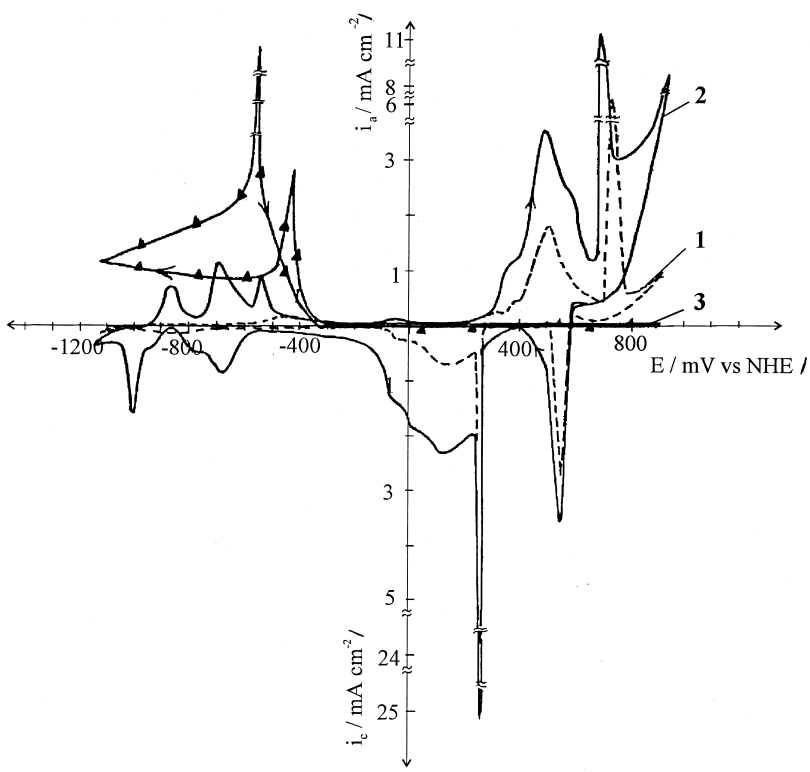

Fig. 7. Linear sweep voltammetric curve for a pure silver electrode (curve 1), Ag-0.44% Tl (curve 2) and pure Tl (curve 3). A potential region from −1100 to +920 mV NHE, $v = 2$ mV s^{-1}.

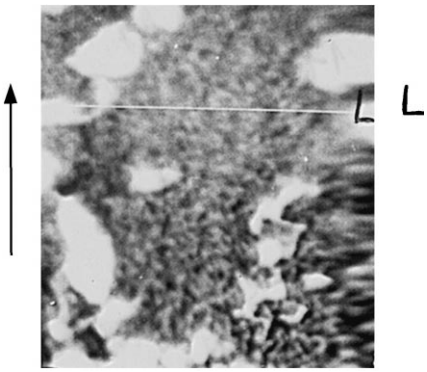

Fig. 8. Grain size of Ag-0.26% Pb (magnification 1400×).

compared with the electrode made of pure silver. AgO formation upon the alloyed electrode is almost at the same potential as for the pure silver electrode. Ag_2O and AgO reduction occurs at potentials for 40 mV and 60 mV more negative then for pure silver, respectively.

The structure of pure silver and silver alloys were characterized by the electron microscope. The grain size of pure silver is about 1 mm and with addition of Pb becomes remarkably smaller, i.e., about 0.02 mm. Inside the grain there is a dendritic segregation of lead and eutectic mixture of silver and lead (according to the constitutional diagram and characterization by the electron microscope). The solubility of lead in alloys is 1.5%, that follows from its constitutional diagram. The lower solubility of Pb may be the reason for dendritic segregation, another reason might be the non-equilibrium conditions of metal casting and cooling, which are not uniform.

Thallium solubility in silver is about 4.2% and arises without eutectic structure, that results from a constitutional diagram of Ag–Tl. The grain size is about 0.005 mm. Many deep holes exist on the boundaries and within the grains. Probably, the grain boundary is very active for electrochemical reactions, i.e., oxide formation. In order to prove such a suggestion, the surface of charged electrode was also characterized. The electrode Ag-0.44% Tl was charged galvanostatically with current density of 5 mA cm^{-2} and then micrographs was taken. Deep holes on the

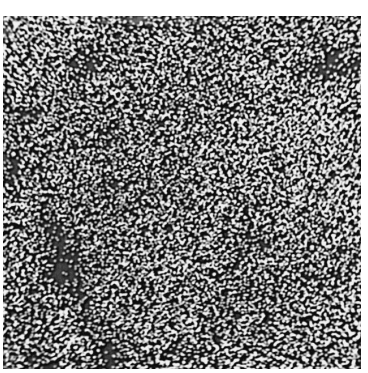

Fig. 9. Distribution of Pb in Ag–Pb grain (magnification 1400×).

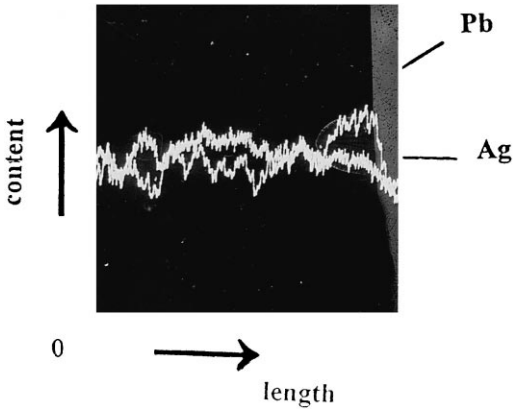

Fig. 10. Content of Pb and Ag in Ag–Pb grain. Upper curve is for content of Pb and lower curve for Ag (magnification 1400×).

boundaries and within the grain could be observed. The same experiment is done with Ag–Pb electrode and then micrographs was taken (see Fig. 8). As the consequence of that oxidation process, the following concentrations of Pb and Tl, 15 ppm cm^{-3} and 9 ppm cm^{-3}, respectively, were detected into the electrolyte.

One Ag–Pb grain is shown in Fig. 8. Photo-microimage is made by the electronic microscope. The distribution of lead within the same grain is shown on a roentgenogram picture (Fig. 9). In the next photo-images (see Fig. 10) the content of lead and silver along L line is shown (position L line is shown in Fig. 8). The silver content is presented with line of smaller oscillations. Peak for the higher content of Pb appeared on the site of the grain boundary.

4. Discussion

Silver alloys were tested by linear sweep voltammetry in a wide potential range. There were no qualitative changes. It means that no new peaks were obtained on an alloyed electrode during silver oxides formation and their corresponding reduction potentials. However, the intensities of silver oxide peaks were higher or smaller than oxide peaks for a pure silver electrode depending on the additive concentration.

By alloying silver with Tl, Pb, Ge, Sb and P, the electrode capacity is increased. However, when silver is alloyed with In, the capacity of such an electrode is decreased. The reason for the increased capacity of such an electrode, in the first case, is a results from its more intense formation of silver oxides. Oxide thickness increases during its formation. Therefore, silver(I)oxide or generally a surface of an electrode becomes more porous.

Structures of alloyed electrodes Ag–Pb or Ag–Tl are not homogeneous. The grain size is decreased by silver alloying. As it was stressed earlier, the concentration of

alloying component is significantly increased on site of the grain boundary, but within the grain the dendritic segregation of alloying component has been found. Therefore, silver on the grain boundary produce dislocations and vacancies. Electrodes with such surfaces are very convenient for electrochemical reactions. Based upon results obtained, in the present work, the concentration of alloying component, Pb, arises on a grain boundary (Fig. 10). Stationary potential of an alloyed electrode indicates that oxidation occurs even at more negative potentials. This is confirmed by linear sweep voltammetry curves in the potential region of −800 to −400 mV NHE. At those potentials Tl and Pb are first oxidized probably into TlOH and $Pb(OH)_2$, and silver later appears oxidized. On the sites where Tl and Pb are oxidized the surface arises more porous. Therefore, the real current density is lowered and the formation of silver oxide occurs at more negative potential. However, when the alloying component is In, the electrode surface is covered with its oxidation product, i.e., $In(OH)_2$, which is less soluble than $Tl(OH)_2$. In that case, the effect of formerly increased the surface area is now suppressed by covering it with $In(OH)_2$ which makes the whole surface less active. The concentration of a soluble alloying component metal ions, near an electrode surface, increased until the saturation has been reached. The solubility of Tl, Pb and In hydroxides is decreased when saturation is reached.

Alloying components can also react with silver oxide (see Eq. (1))

$$2AgO + 2Tl + H_2O = Ag_2O + TlOH \quad (1)$$

A decomposition reaction rate is increased by increasing the surface roughness. The self-discharge of the electrode alloyed with In, Tl and Pb is higher than self-discharge for pure silver. Only for silver alloys with 0.5% In or 0.5% Tl, the self-discharge is similar to that of pure silver.

The increased capacity of alloyed silver electrodes could be explained based on the effect of alloying component on the conductivity of semiconducting silver(I)oxide. With the increase of the deformation of the silver crystal structure by alloying [9], the self-diffusion of a silver ion and the conductivity arise improved as well. Such experimental and theoretical evidence is discussed in the second part of the same study [10]. The oxide formation over voltage for alloyed electrodes is lower than oxide formation over voltage for pure silver electrodes, as it has been observed in the present paper.

5. Conclusions

Silver electrode capacity for oxide formation is improved for 150% by specific alloying. Contents of alloying components Tl, Pb, P, Ge, In and Sb were less than 1%. Thallium (0.44%) and lead (0.44%) in the binary alloys have exhibited the positive effects and the highest influence on electrode capacity. Other alloys also have their positive effects, but increased values of electrode capacity are not so high. Negative influence on the electrode capacity exhibits only Ag–In alloy.

Alloying components make smaller silver grains sizes and its concentration increases along the grain boundary. During electrochemical oxidation of an electrode, the first product of oxidation just represents the alloying component itself. The solubility of hydroxides of alloying components is satisfactory. The site formerly occupied by the alloying component becomes free, and the electrode surface arises more porous. The increase in the electrode surface area consequently produces a decrease in the current density and increase in the oxide formation also.

Acknowledgements

Financial support for this study was provided by the scientific Found of Serbia.

References

[1] D.T. Grozdić, et al., Electrochemical characteristics of binary silver alloys in alkaline solution, 37 ISE Maastriht, 1987, 532–533.
[2] J.J. Lander, Sealed Zinc–silver Oxide Batteries, Proc. 15th Annual Power Sources Conf., 1961, 77–80.
[3] A.P. Malachevsky, R. Jasinsky, J. Electrochem. Soc. 114 (1967) 1239.
[4] A.P. Malachevsky, R. Jasinsky, J. Electrochem. Soc. 114 (1967) 1258.
[5] S. Yoshizawa, Z. Takeharo, Denki Kagaku 32 (3) (1964) 197, CA 197, 62374h.
[6] J. Rhyne, Silver Oxide–zinc Battery Program, Wad Technical report 61036 contract NA-AF., 33 (600)-41600, 1961.
[7] D.T. Grozdić, PhD Thesis, University SPLIT, 1987,.
[8] J. Garche, T.D. Grozdić, K. Wiesener, J. Mrha, Silver oxide electrode on base of alloy, 25-09-1986, DD-HO1M/294 6570.
[9] B.N. Hannay, Solid-State Chemistry, Pub. 'MIR' Moskva, 1971.
[10] T.D. Grozdić, D. Stojić, Charge transport in silver/silver oxide, OH layer, Mechanism, to be published (ibid).